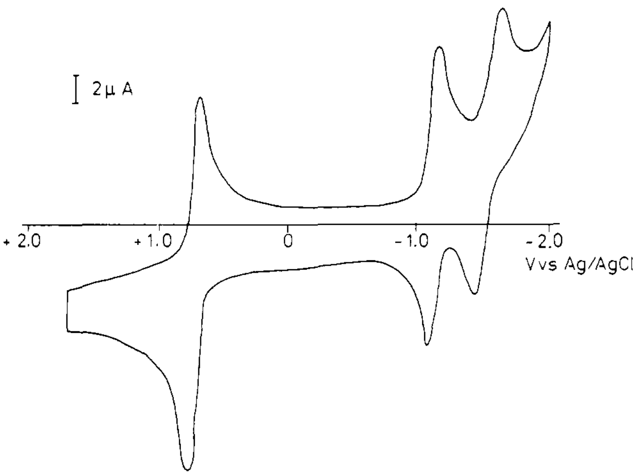

Figure 10. Cyclic voltammogram of **8** in CH_3CN (0.1 M $[n\text{-}Bu_4N]PF_6$) at an Au electrode at scan rate 200 mV s^{-1}.

and −2.10 V vs Fc^+/Fc, which correspond to the processes in eq 2.

$$V^{III}V^{IV} \underset{E^1_{1/2}}{\overset{+e^-}{\underset{-e^-}{\rightleftharpoons}}} V^{III}{}_2 \underset{E^2_{1/2}}{\overset{+e^-}{\underset{-e^-}{\rightleftharpoons}}} V^{III}V^{II} \underset{E^3_{1/2}}{\overset{+e^-}{\underset{-e^-}{\rightleftharpoons}}} V^{II}V^{II} \qquad (2)$$

Substitution of the acetato bridges in $[L_2V_2(\mu\text{-}O)(\mu\text{-}O_2CCH_3)_2]^{2+}$ by benzoato bridges brings about an anodic shift of $E^1{}_{1/2}$ and $E^2{}_{1/2}$ by 220 and 30 mV. Similar effects have been reported for the corresponding (μ-oxo)bis(carboxylato)diruthenium(III) complexes.[32]

Summary. We have shown in this study that the octahedral monomeric complexes **1** and **2** containing the blocking tridentate macrocycle L and three labile unidentate ligands such as Cl^- or $CF_3SO_3^-$ are hydrolyzed in aqueous solution under anaerobic conditions to form binuclear species containing the $[V\text{–}O\text{–}V]^{4+}$ core. In **6**–**8** the two V(III) centers are intramolecularly ferromagnetically coupled. Electrochemically these complexes may be reversibly oxidized or reduced, generating the mixed-valence $V^{III}V^{IV}$ and $V^{III}V^{II}$ binuclear complexes. The reaction of NH_4VO_3 or V_2O_5 with L in CH_3CN/H_2O yields the novel neutral complex **9**, which is protonated in acidic solution at the *cis*-VO_2 core to give the *cis*-VO(OH) unit. This reaction emphasizes nicely the analogy between the *cis*-VO_2 functionality and organic carboxylates.

Acknowledgment. We are grateful to Drs. J. J. Girerd and J. Bonvoisin (Université Paris-Sud) for the low-temperature magnetic susceptibility measurements. The Fonds der Chemischen Industrie has generously supported this work.

Registry No. **1**, 112087-96-4; **2**, 123812-88-4; **3**, 123812-89-5; **4**, 123812-90-8; **5**, 123812-91-9; **5**$^+$, 123880-71-7; **6**, 123812-92-0; **6**$^+$, 123812-98-6; **7**, 123812-93-1; **8**, 123812-94-2; **9**, 123812-95-3; **10**, 123812-97-5; $[L_2V_2(\mu\text{-}O)(\mu\text{-}O_2CCH_3)_2]I_2\cdot 2H_2O$, 106264-13-5; $[L_2V_2(acac)_2O]^{3+}$, 123834-35-5; $[L_2V_2(acac)_2O]^+$, 123812-99-7; $[L_2V_2O(C_6H_5CO_2)_2]^{3+}$, 123813-00-3; $[L_2V_2O(C_6H_5CO_2)_2]^+$, 123813-01-4; $[L_2V_2O(C_6H_5CO_2)_2]$, 123813-02-5.

Supplementary Material Available: For complexes **7**, **9**, and **10**, listings of crystallographic data, bond lengths and bond angles, anisotropic thermal parameters, and calculated positions of hydrogen atoms and their thermal parameters (11 pages); observed and calculated structure factor tables (48 pages). Ordering information is given on any current masthead page.

Contribution from the Department of Chemistry,
University of Otago, P.O. Box 56, Dunedin, New Zealand

Orthophosphate Complexes of Cobalt(III). *trans*-$[Co(en)_2(OH_2)(OPO_3H)]ClO_4\cdot{}^1/_2H_2O$ and Its Properties in Aqueous Solution

Nicola E. Brasch, David A. Buckingham,* Jim Simpson, and Ian Stewart

Received April 25, 1989

trans-$[Co(en)_2(OH_2)(OPO_3H)]ClO_4\cdot{}^1/_2H_2O$ has been prepared, and its properties in aqueous solution have been investigated as a function of pH (electronic spectra ϵ (λ), 48 mol^{-1} dm^3 cm^{-1} (570 nm), 69 (359) at pH 1; ^1H and ^{31}P NMR spectra; acidity constants, $pK_{a1} = 3.1$, $pK_{aq} = 6.6$, $pK_{a2} = 9.27$). An X-ray crystallographic study of *trans*-$[Co(en)_2(OH_2)(OPO_3H)](ClO_4)\cdot{}^1/_2H_2O$ [monoclinic, $P2_1/c$, $a = 13.633$ (7) Å, $b = 13.540$ (5) Å, $c = 17.331$ (8) Å, $\beta = 110.65$ (4)°, $Z = 8$] confirms the trans orientation of the monodentate phosphato and aqua ligands. Crystal data collection $4° < 2\theta < 45°$ at 163 K on a Nicolet P3 diffractometer gave 3900 reflections of which 1938 had $I > 2\sigma(I)$. The structure was solved by Patterson methods, and weighted isotropic refinement of all non-hydrogen atoms from the two distinct molecules in the asymmetric unit converged to give $R = 0.142$. Kinetic and equilibrium relationships at 25 °C and 1.0 mol dm^{-3} $NaClO_4$ are as follows. (1) For reactions observed at pH <3: *trans*-$[Co(en)_2(OH_2)(OPO_3H_2)]^{2+}$ ($pK_{a1} = 3.17$) → *cis*-$[Co(en)_2(OH_2)(OPO_3H_2)]^{2+}$ ($pK_{a1} = 3.10$), $k_0{}^t = 4 \times 10^{-5}$ s^{-1}; $[Co(en)_2(O_2P(OH)_2)]^{2+}$ chelate ($pK_a = -0.15$) → *cis*-$[Co(en)_2(OH_2)(OPO_3H_2)]^{2+}$, $k_0{}^{ch} = 1.67$ s^{-1}. (2) For reactions at pH 3–7: *trans*-$[Co(en)_2(OH_2)(OPO_3H)]^+$ ($pK_{aq} = 6.6$) $\rightleftarrows$ *cis*-$[Co(en)_2(OH_2)(OPO_3H)]^+$ ($pK_{aq} = 6.75$), $k_1{}^t = 2.08 \times 10^{-4}$ s^{-1}, $k_1{}^{cis/trans} \sim 0$, $K_1{}^{trans/cis} \sim 0$; $[Co(en)_2(O_2PO(OH))]^+$ chelate ($pK_a = 4.25$) $\rightleftarrows$ *cis*-$[Co(en)_2(OH_2)(O_2PO_3H)]^+$, $k_1{}^{ch} = 5.7 \times 10^{-3}$ s^{-1}, $k_1{}^{cis/trans} = 2.2 \times 10^{-4}$ s^{-1}, $K_1{}^{ch/cis} \simeq 0.04$. (3) For reactions at pH 8–10: *trans*-$[Co(en)_2(OH)(OPO_3H)]$ ($pK_{a2} = 9.27$) $\rightleftarrows$ *cis*-$[Co(en)_2(OH)(OPO_3H)]$ ($pK_{a2} = 9.40$), $k_2{}^t = 2 \times 10^{-5}$ s^{-1}, $k_2{}^{cis/trans} = 1 \times 10^{-5}$ s^{-1}, $K_2{}^{trans/cis} \simeq 0.5$; $[Co(en)_2(O_2PO_2)]$ chelate $\rightleftarrows$ *cis*-$[Co(en)_2(OH)(OPO_3H)]$, $k_2{}^{ch} = 2.2 \times 10^{-5}$ s^{-1}, $k_2{}^{cis/ch} = 6 \times 10^{-4}$ s^{-1}, $K_2{}^{ch/cis} \simeq 25$. (4) For strongly alkaline conditions, pH >10: *trans*-$[Co(en)_2(OH)(OPO_3)]^-$ $\rightleftarrows$ *cis*-$[Co(en)_2(OH)(OPO_3)]^-$, $k_3{}^t \simeq 1.3 \times 10^{-6}$ s^{-1}, $k_3{}^{cis/trans} \simeq 5.4 \times 10^{-6}$ s^{-1}, $K_3{}^{trans/cis} \simeq 4$; $[Co(en)_2(O_2PO_2)] + OH^-$ $\rightleftarrows$ *cis*-$[Co(en)_2(OH)(OPO_3)]^-$, $k_3{}^{ch} = 1.75 \times 10^{-2}$ mol^{-1} dm^3 s^{-1}, $k_3{}^{cis/ch} = 7.5 \times 10^{-5}$ s^{-1}, $K_3{}^{ch/cis} = 4.3 \times 10^{-3}$ mol dm^{-3}.

Introduction

This study describes the preparation and isolation of *trans*-$[Co(en)_2(OH_2)(OPO_3H)]ClO_4\cdot{}^1/_2H_2O$ and reports its solid-state structure and its equilibrium and kinetic properties in aqueous solution over the pH range 0–12.

In a previous communication, we noted, by making use of ^{31}P NMR spectroscopy, the presence of a new species in addition to *cis*-$[Co(en)_2(OH)(OPO_3)]^-$ when alkaline aqueous solutions of the four-membered phosphate chelate $[Co(en)_2(O_2PO_2)]$ were allowed to stand at room temperature.[1] This was thought to be the trans isomer and suggested to us that opening up of the chelate under such conditions might be more complicated than was originally thought by Lincoln and Stranks.[2,3] Those authors in-

---

(1) Buckingham, D. A.; Clark, C. R.; Stewart, I. *Aust. J. Chem.* **1989**, *42*, 709.

0020-1669/90/1329-0371$02.50/0

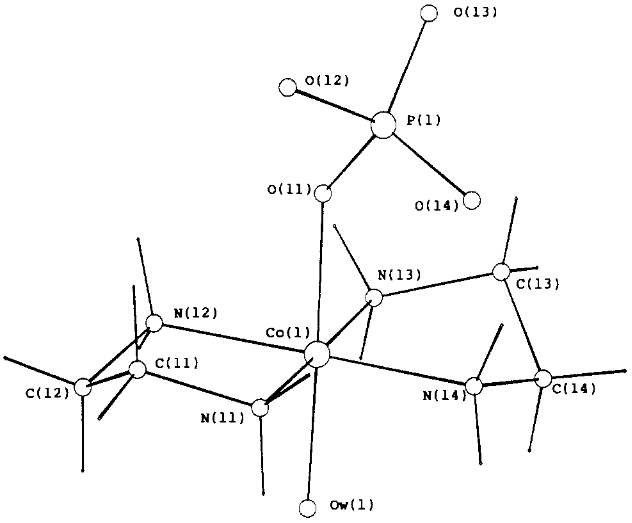

Figure 1. Perspective drawing of one of the two unique *trans*-[Co(en)$_2$(OH$_2$)(OPO$_3$H)]$^+$ cations in the unit cell showing the atom-numbering scheme. Co(1)–O(11) = 1.92 (2) Å; Co(1)–O$_w$(1) = 1.93 (2) Å; Co(1)–N(11) = 1.94 (3) Å; Co(1)–N(12) = 2.100 (2) Å; Co(1)–N(12) = 1.93 (2) Å; Co(2)–N(14) = 1.96 (2) Å; P(1)–O(11) = 1.51 (2) Å; P(1)–O(12) = 1.63 (2) Å; P(1)–O(13) = 1.51 (2) Å; P(1)–O(14) = 1.53 (7) Å; O(11)–Co(1)–O$_w$(1) = 173.6 (9)°.

terpreted equilibrium and kinetic data in terms of the chelate and various protonated forms of the cis-monodentate complex only and specifically stated a failure to detect the trans isomer.[3,4] It has also been subsequently shown that cleavage of the chelate in mild or strong alkali occurs only by substitution at the metal[1,5] (whereas Lincoln and Stranks had proposed some O–P bond fission[2]), and this enhances the possibility of direct formation of the trans-monodentate isomer from the chelate.

It was therefore the purpose of this study to investigate this system in a little more detail, particularly with regard to relationships existing between the cis- and trans-monodentate species and with the four-membered chelate. The study parallels in some respects our previous investigations of the five-membered oxalate system[6,7] and completes an overall study of several oxyanion chelates of cobalt(III).[8] In due respect to Lincoln and Stranks, it should be pointed out that this study could not have been carried out without the extensive use of ^{31}P NMR spectroscopy, and such facilities were not available to those authors in their excellent detailed investigations.[2-4,9,10]

Experimental Section

[Co(en)$_2$(O$_2$PO$_2$)] was prepared according to a published procedure[2] using *trans*-[Co(en)$_2$Br$_2$]Br instead of the chloro complex. It was recrystallized by dissolution in warm dilute HClO$_4$ (~40 °C) followed by readjustment to pH ~8. On standing overnight (~10 h) at room temperature, the uncharged chelate complex slowly crystallized. *cis*-[Co(en)$_2$(OH$_2$)(OPO$_3$H$_2$)](ClO$_4$)$_2$ was prepared as previously reported[2] for the *cis*-[Co(en)$_2$(OH$_2$)(OPO$_3$H)](ClO$_4$) salt. In our hands, the diprotonated phosphato complex crystallized under the reported conditions.

Table I. Final Atomic Positional and Thermal Parameters for *trans*-[Co(en)$_2$(OH$_2$)(OPO$_3$H)](ClO$_4$)·$^1/_2$H$_2$O

atom	*x*/*a*	*y*/*b*	*z*/*c*	U_{11}/Å^2
Co(1)	−0.2163 (3)	0.2014 (3)	0.0417 (2)	0.008 (1)
P(1)	0.3885 (6)	0.3444 (6)	0.0152 (5)	0.009 (2)
O(11)	0.343 (2)	0.246 (2)	0.028 (1)	0.020 (5)
O(12)	0.386 (2)	0.348 (2)	−0.080 (1)	0.018 (5)
O(13)	0.503 (2)	0.346 (2)	0.070 (1)	0.017 (5)
O(14)	0.323 (2)	0.432 (2)	0.027 (1)	0.015 (5)
O$_w$(1)	0.099 (2)	0.145 (2)	0.063 (1)	0.013 (5)
N(11)	0.129 (2)	0.256 (2)	−0.064 (2)	0.015 (6)
C(11)	0.141 (2)	0.196 (2)	−0.133 (2)	0.004 (6)
C(12)	0.147 (3)	0.084 (3)	−0.100 (2)	0.020 (8)
N(12)	0.230 (2)	0.082 (2)	−0.022 (1)	0.009 (6)
N(13)	0.306 (2)	0.147 (2)	0.146 (2)	0.011 (6)
C(13)	0.345 (2)	0.229 (2)	0.211 (2)	0.017 (8)
C(14)	0.243 (3)	0.292 (3)	0.193 (2)	0.024 (9)
N(14)	0.201 (2)	0.321 (2)	0.101 (1)	0.009 (6)
Cl(1)	0.4602 (6)	0.0276 (6)	0.8683 (5)	0.017 (2)
O(1)	0.483 (2)	−0.074 (2)	0.863 (2)	0.057 (9)
O(2)	0.356 (2)	0.034 (2)	0.867 (2)	0.043 (7)
O(3)	0.467 (2)	0.079 (2)	0.798 (2)	0.031 (6)
O(4)	0.533 (4)	0.073 (4)	0.938 (3)	0.11 (2)
Co(2)	0.7143 (3)	0.2897 (3)	−0.0098 (2)	0.009 (1)
P(2)	0.8387 (6)	0.1480 (6)	−0.0868 (5)	0.009 (2)
O(21)	0.747 (2)	0.172 (2)	−0.059 (1)	0.009 (5)
O(22)	0.931 (2)	0.214 (2)	−0.046 (1)	0.011 (5)
O(23)	0.861 (2)	0.036 (2)	−0.073 (1)	0.012 (5)
O(24)	0.804 (2)	0.176 (2)	−0.185 (1)	0.012 (5)
O$_w$(2)	0.674 (2)	0.400 (2)	0.041 (1)	0.009 (5)
N(21)	0.579 (2)	0.293 (2)	−0.105 (2)	0.018 (6)
C(21)	0.587 (3)	0.384 (3)	−0.154 (2)	0.022 (8)
C(22)	0.693 (2)	0.391 (2)	−0.160 (2)	0.000 (6)
N(22)	0.771 (2)	0.380 (2)	−0.072 (1)	0.006 (6)
N(23)	0.849 (2)	0.285 (2)	0.077 (2)	0.015 (6)
C(23)	0.852 (3)	0.198 (3)	0.136 (2)	0.029 (9)
C(24)	0.740 (2)	0.203 (3)	0.142 (2)	0.015 (7)
N(24)	0.664 (2)	0.199 (2)	0.057 (1)	0.012 (6)
Cl(2)	−0.0011 (7)	0.0099 (7)	0.3443 (6)	0.029 (2)
O(5)	0.095 (3)	0.018 (3)	0.418 (2)	0.07 (1)
O(6)	0.031 (4)	0.034 (4)	0.274 (3)	0.15 (2)
O(7)	−0.073 (2)	0.088 (2)	0.334 (2)	0.061 (9)
O(8)	−0.041 (3)	−0.085 (3)	0.325 (2)	0.07 (1)
O$_w$(3)	0.252 (2)	0.061 (2)	0.292 (1)	0.022 (6)

***trans*-[Co(en)$_2$(OH$_2$)(OPO$_3$H)](ClO$_4$)·$^1/_2$H$_2$O** was prepared as follows: [Co(en)$_2$(O$_2$PO$_2$)] (5 g) dissolved in warm water (250 cm^3, ~40 °C) was taken to pH ~12 by adding solid NaOH and the solution left for 1 week at 25 °C with periodic checks to maintain the pH. (Alternatively 5 g of *cis*-[Co(en)$_2$(OH$_2$)(OPO$_3$H$_2$)](ClO$_4$)$_2$ in 150 cm^3 of water at pH ~12 may be used.) The pH was then adjusted to ~10 (1 M HClO$_4$) and the volume reduced to ~60 cm^3 by rotary evaporation. The pH was then further reduced to ~5, when adding solid NaClO$_4$·H$_2$O and cooling in ice caused purple crystals to deposit. These were collected and washed with ice-cold aqueous NaClO$_4$ followed by MeOH. Recrystallization was effected by dissolution in cold water, quickly filtering, adding solid NaClO$_4$·H$_2$O, and cooling as above. Anal. Calcd for [Co(en)$_2$(OH$_2$)(OPO$_3$H)]ClO$_4$·$^1/_2$H$_2$O: C, 12.0; H, 5.0; N, 14.0; Cl, 8.8; P, 7.7. Found: C, 12.0; H, 5.2; N, 13.4; Cl, 9.0; P, 7.7.

Crystals so obtained were small and weakly diffracting. An X-ray data set was collected on a Nicolet P3 diffractometer and proved to be of poor (cf. Abstract), but sufficient, quality to allow solution of the structure and confirmation of the trans geometry (Figure 1). A second data set from a new crystal from another preparation showed no improvement. Further refinement will require a larger crystal, but due to the relatively rapid isomerization to the cis geometry under slightly acidic conditions, this may be difficult to obtain. Table I lists final atom positions for the two unique molecules in the unit cell.

Spectrometric and pH Measurements. Visible–UV spectra and kinetic data were recorded by using a Cary 219 spectrophotometer at 25 °C. ^{1}H and ^{31}P NMR spectra were obtained by using a Varian VXR 300 spectrometer and 5-mm (^{1}H, 299.9 MHz) or 10-mm (^{31}P, 121.4 MHz) probes thermostated to 25 °C. Solutions were made up in either D$_2$O (^{1}H) or 20% D$_2$O–80% H$_2$O (^{31}P) by using internal TPS-*d*$_4$ (3-(trimethylsilyl)-1-propionic-*d*$_4$ acid, sodium salt) and external 0.1 M H$_3$PO$_4$ as references, respectively. A 3-s time delay between acquisitions was found to be sufficient to completely relax the ^{31}P nuclei under all pH conditions. Integrated absorptions were then used to compare concentrations. When relative concentrations were not required (e.g. kinetic data) 1- or 2-s time delays were used.

pH measurements and titrations were made by using a digital Radiometer pHM 62 meter equipped with an ABU-12 autoburet and TTT-60 titrator.

Acidity Constants. The $K_{a,aq}$ and K_{a2} values were determined by adding to *trans*-[Co(en)$_2$(OH$_2$)(OPO$_3$H)]ClO$_4$·$^1/_2$H$_2$O (157 mg) dis-

---

(2) Lincoln, S. F.; Stranks, D. R. *Aust. J. Chem.* **1968**, *21*, 37.
(3) Lincoln, S. F.; Stranks, D. R. *Aust. J. Chem.* **1968**, *21*, 57.
(4) Lincoln, S. F.; Stranks, D. R. *Aust. J. Chem.* **1968**, *21*, 1745.
(5) Jones, D. R.; Lindoy, L. F.; Sargeson, A. M. *J. Am. Chem. Soc.* **1983**, *105*, 7327.
(6) Miskelly, G. M.; Clark, C. R.; Simpson, J.; Buckingham, D. A. *Inorg. Chem.* **1983**, *22*, 3237.
(7) Miskelly, G. M.; Clark, C. R.; Buckingham, D. A. *J. Am. Chem. Soc.* **1986**, *108*, 5202.
(8) Buckingham, D. A.; Clark, C. R.; Miskelly, G. M. *Comments Inorg. Chem.* **1988**, *7*, 171.
(9) Lincoln, S. F.; Stranks, D. R. *Aust. J. Chem.* **1968**, *21*, 67.
(10) Lincoln, S. F.; Stranks, D. R. *Aust. J. Chem.* **1968**, *21*, 1733.

solved in 50 cm^3 of 1.0 M $NaClO_4$ at 25 °C 250-μL aliquots of 0.2 M NaOH/0.8 M $NaClO_4$ and recording the pH after each addition. K_{a1} was similarly determined by adding to 785.1 mg of complex dissolved in 20 cm^3 of 1.0 M $NaClO_4$ 250-μL aliquots of 1.0 M $HClO_4$ solution. Corrections for volume changes were made, and calculations were carried out, according to the procedure of Albert and Serjeant.[11] Additions were carried out as quickly as possible to minimize isomerization to the cis complex.

^{31}P NMR Kinetic Measurements. To obtain the solutions used, ~60 mg of $[Co(en)_2(O_2PO_2)]$, or ~75 mg of *trans*-$[Co(en)_2(OH_2)(OPO_3H)]ClO_4 \cdot H_2O$, or ~100 mg of *cis*-$[Co(en)_2(OH_2)(OPO_3H_2)](ClO_4)_2$ was dissolved in 2.5–3.5 cm^3 of H_2O, 20% by volume of D_2O added, solid MES, CAPS, TAPS, or $NEt_3 \cdot HCl$ buffer and $NaClO_4$ added to make the solution 0.1 M in buffer and 0.9 M in $NaClO_4$ respectively, and the pH adjusted to the required value by adding 1.0 M NaOH (pH Stat). Then, 3.1 cm^3 of this solution was transferred to the 10-mm NMR tube and data collection begun as quickly as possible (~10 min). A total of 256 or 512 acquisitions were accumulated, with a predetermined time delay (2.0 or 3.0 s) between acquisitions (acquisition times 0.753, 1.004, or 1.517 s; pulse widths 5.4 (27.8°) or 5.9 μs (30.3°)).

^{31}P NMR Equilibrium Measurements. To 4.0 g of *cis*-$[Co(en)_2(OH_2)(OPO_3H_2)](ClO_4)_2$ dissolved in H_2O (160 cm^3) was added 19.76 g of solid $NaClO_4 \cdot H_2O$ (0.9 M) and the solution divided into four equal parts. To each was added sufficient solid buffer (TES, TAPS, CAPS, or $NEt_3 \cdot HCl$) to make it 0.1 M in buffer, and the pH was brought to the desired value by adding 1.0 M NaOH. Samples (5 cm^3) were withdrawn at each pH and stored in a thermostated bath at 25 °C. When appropriate (1, 2, or 5 weeks), 20% by volume of D_2O was added and the ^{31}P NMR spectrum recorded (512 or 1024 acquisitions; 3-s time delay; pulse width 10 μs (51.4°)). The pH was checked before the addition of D_2O.

Results

1. Preparation, Isolation, and Properties of *trans*-$[Co(en)_2(OH_2)(OPO_3H)]ClO_4 \cdot {}^1/_2H_2O$.

The *trans* monodentate orthophosphate complex was prepared by allowing an aqueous solution of the chelate to equilibrate for about 1 week at pH ~12, 25 °C. Under this condition, the overall equilibrium favors the trans isomer (by about 4:1 over the cis; see below), but some total hydrolysis to free phosphate and $[Co(en)_2(OH)_2]^+$ also occurs (eq 1). Further hydrolysis is found at longer times, but even this eventually reaches equilibrium with the two monodentate and single chelate species.

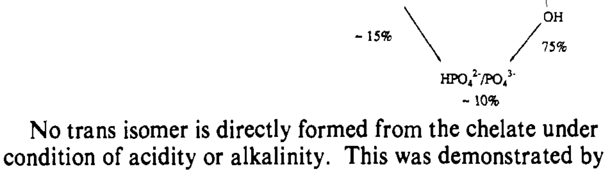

(1)

No trans isomer is directly formed from the chelate under any condition of acidity or alkalinity. This was demonstrated by ^{31}P NMR spectroscopy where the signal for the cis-monodentate isomer always appears first followed by that for the trans complex. It was shown by analysis of the kinetic data (see below) that the sequence chelate → cis → trans → HPO_4^{2-}/PO_4^{3-} is followed under all alkaline conditions (pH >7). At equilibrium, no ^{31}P NMR evidence for the trans complex could be found for pH <6.

Reduction of the solution volume in the preparative experiment, adjustment of the pH to ~5, and addition of $NaClO_4$ resulted in crystalline, mauve purple *trans*-$[Co(en)_2(OH_2)(OPO_3H)]ClO_4 \cdot {}^1/_2H_2O$. The cis isomer does not crystallize from this solution, and the yield can be increased by cooling. However, recrystallization from cold water (by addition of solid $NaClO_4$) must be effected quickly to avoid contamination by the cis isomer since isomerization is relatively rapid in neutral solution (see below).

Once contaminated, the pure trans complex can only be recovered with great difficulty and with considerable loss of material. The solid trans complex is stable toward isomerization or chelation for at least reasonable periods of time at ambient temperatures (more than 6 months at ~18 °C).

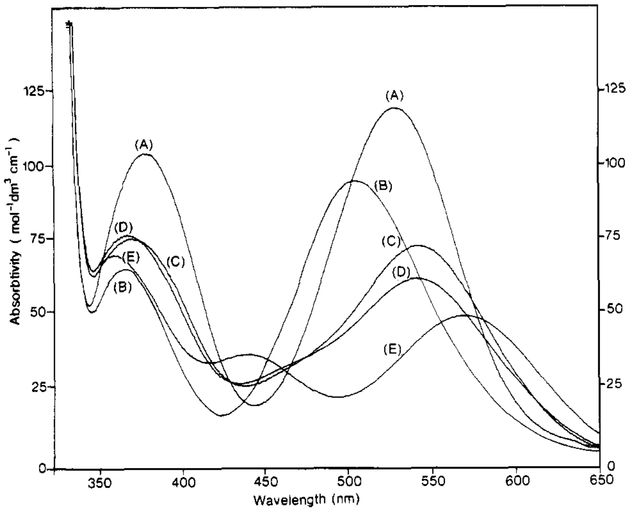

Figure 2. Visible–UV absorption spectra (ϵ (λ, nm), mol^{-1} dm^3 cm^{-1}): (A) chelate $[Co(en)_2(O_2PO_2)]$ in 1.0 M $NaNO_3$ (115 (528), 100 (378)); (B) *cis*-$[Co(en)_2(OH_2)(OPO_3H_2)]^{2+}$ in 0.1 M HNO_3/1.0 M $NaNO_3$ (94 (504), 64 (366)); (C) *trans*-$[Co(en)_2(OH)(OPO_3)]^-$ at pH 12.0 in 0.1 M $NaNO_3$ (72 (542), 75 (370)); (D) *trans*-$[Co(en)_2(OH)(OPO_3H)]$ at pH 8.1 in 0.1 M $NaNO_3$ (63 (542), 76 (367)); (E) *trans*-$[Co(en)_2(OH_2)(OPO_3H_2)]^{2+}$ in 0.1 M HNO_3/1.0 M $NaNO_3$ (48 (570), 69 (359)).

The easily soluble trans salt gives a typical "trans" absorption spectrum in acid solution (Figure 2E), with the first absorption band being shifted to a longer wavelength compared to that of the cis isomer (B) and having a reduced extinction. This is characteristic of other trans complexes including *trans*-$[Co(en)_2(OH_2)_2]^{3+}$ [12] and *trans*-$[Co(en)_2(OH_2)(OC_2O_3H)]^{2+}$,[6] and the present spectrum in acid solution is remarkably similar to that for *trans*-$[Co(en)_2(OH_2)_2]^{3+}$. The caption to Figure 2 gives extinctions and band maxima for the various protonated species. Related spectra for the cis ions are given in the earlier publication.[1]

Figure 3 gives ^{1}H NMR spectra for *trans*-$[Co(en)_2(OH_2)(OPO_3H_2)]^{2+}$ (A) and *trans*-$[Co(en)_2(OH_2)(OPO_3H)]^+$ (B) together with comparative spectra for the cis-monodentate (C) and chelate (D) complexes. The former show the simplicity and symmetry expected of a trans structure, particularly in the C–H region, whereas the cis-monodentate and chelate complexes give more complex patterns. One set of trans N–H protons shows an unusually large chemical shift on ionization of the first phosphate proton (6.0–5.6 ppm shift), and it is tempting to ascribe this to intramolecular H-bonding between the phosphate anion and a coordinated amine residue. No similar shift occurs with the cis isomer although some improved definition of the overlapping N–H absorptions at 4.5–4.6 ppm (Figure 6C) is observed in this complex at pH ~5 (not shown). Under this latter condition, slow deuteration of the amine sites occurs in both the cis and trans complexes. Many factors are known to be involved in determining N–H proton frequencies in Co(III) complexes,[13] and a detailed analysis of their position in the present complexes lies outside the scope of this study. It is of interest to note however the appearance of the two sets of high-field N–H resonances in the cis isomer and the upfield shift of all N–H resonances in the chelate, whereas the ^{31}P resonance moves downfield on coordination or chelation (see below).

^{31}P NMR spectra (Figure 4) show the anticipated downfield shift on ionization and chelation of the phosphate moiety, but the trans isomer shows somewhat less of a downfield shift than the cis. In neutral to slightly alkaline solution, the two complexes show opposite effects as the pH moves through the pK_a of the coordinated water molecule. Data in Table S1 (supplementary material) are given as a plot of chemical shift vs pH in Figure 5. Ionization of trans water results in substantial shielding of

---

[11] Albert, A.; Serjeant, E. P. In *Ionization Constants of Acids and Bases*; Wiley: New York, 1962.

[12] Bjerrum, J.; Rasmussen, S. E. *Acta. Chem. Scand.* **1952**, *6*, 1265.

[13] Bramley, R.; Brarson, M.; Sargeson, A. M.; Schäffer, C. E. *Inorg. Chem.* **1987**, *26*, 314 and earlier references quoted therein.

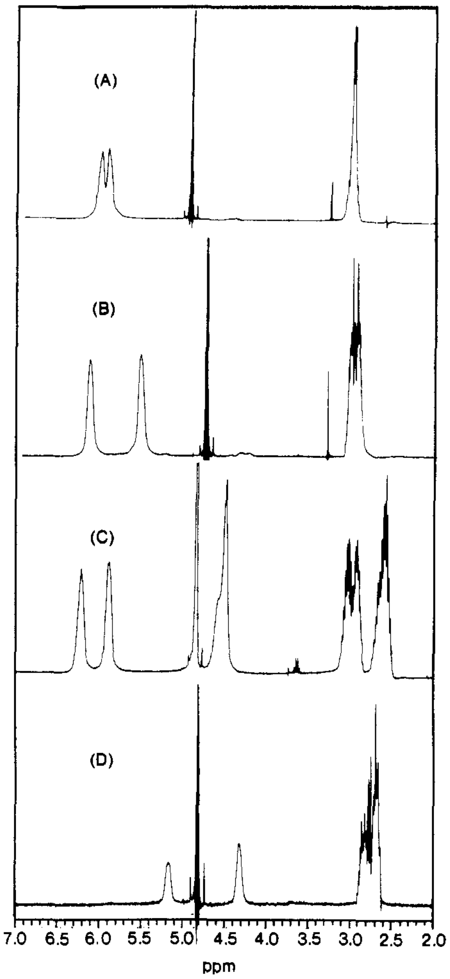

Figure 3. 300-MHz ^1H NMR spectra (ppm referenced to internal TSP at 0.0 ppm): (A) *trans*-$[Co(en)_2(OH_2)(OPO_3H_2)]^{2+}$ in 0.1 M $DClO_4$ (N-H 6.09 (4), 6.01 (4); C-H 3.1 (8)); (B) *trans*-$[Co(en)_2(OH_2)(OPO_3H)]^+$ in D_2O (neutral) (N-H 6.2 (4), 5.58 (4); C-H 3.04 (8)); (C) *cis*-$[Co(en)_2(OH_2)(OPO_3H_2)]^{2+}$ in 0.1 M $DClO_4$ (N-H 6.23 (2), 5.91 (2), 4.5-4.6 (4); C-H 3.0 (4), 2.6 (4)); (D) chelate $[Co(en)_2(O_2PO_2)]$ in D_2O (N-H 5.16 (4), 4.31 (4); C-H 2.65-2.8 (8)).

the P atom whereas ionization of cis water results in increased deshielding. This could arise in the former instance by transmission of charge density from coordinated OH^- to the trans-P atom, whereas in the cis complex the coordinated OH^- ligand is in a position to H-bond to the remaining acidic proton of the adjacent phosphate group, thereby removing charge density from the P center. The resulting structure has some of the elements of "chelation" about it. When the final phosphate proton is removed, both complexes again show similar ^{31}P chemical shifts, demonstrating that there is no intrinsic difference between ^{31}P resonances for the cis and trans geometries.

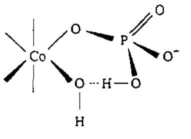

Table II gives pK_{a1}, pK_{aq}, and pK_{a2} values for the equilibria

$$trans\text{-}[Co(en)_2(OH_2)(OPO_3H_2)]^{2+} + H_2O \xrightleftharpoons{K_{a1}} trans\text{-}[Co(en)_2(OH_2)(OPO_3H)]^+ + H_3O^+ \quad (2)$$

$$trans\text{-}[Co(en)_2(OH_2)(OPO_3H)]^+ + H_2O \xrightleftharpoons{K_{aq}} trans\text{-}[Co(en)_2(OH)(OPO_3H)] + H_3O^+ \quad (3)$$

$$trans\text{-}[Co(en)_2(OH)(OPO_3H)] + H_2O \xrightleftharpoons{K_{a2}} trans\text{-}[Co(en)_2(OH)(OPO_3)]^- + H_3O^+ \quad (4)$$

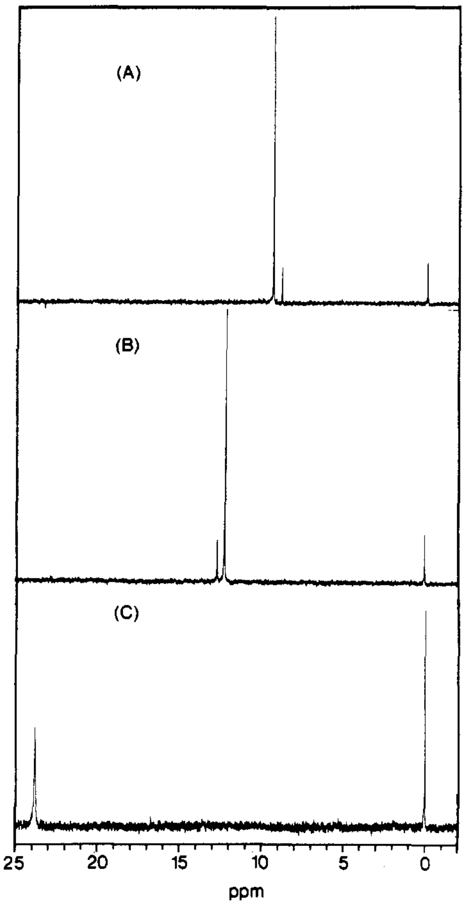

Figure 4. 300-MHz ^{31}P NMR spectra (ppm referenced to external 0.1 M H_3PO_4 at 0.0 ppm; 20% D_2O in H_2O): (A) *trans*-$[Co(en)_2(OH_2)(OPO_3H_2)]^{2+}$ containing a trace of the cis isomer in 0.2 M HNO_3 (trans 9.42 ppm, cis 8.90 ppm); (B) *trans*-$[Co(en)_2(OH_2)(OPO_3H)]^+$ containing a trace of the cis isomer in nearly neutral solution (pH 5.5; cis 12.65 ppm, trans 12.20 ppm); (C) chelate $[Co(en)_2(O_2PO_2)]$ in neutral solution (pH 7; 23.80 ppm).

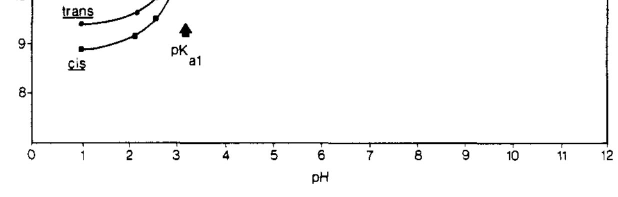

Figure 5. ^{31}P NMR frequencies (ppm from external 0.1 M H_3PO_4 reference) for the trans- and cis-monodentate phosphate complexes as a function of pH (20% D_2O/H_2O solutions, 25 °C). Data are from Table S1 (supplementary data).

together with those previously found for the similar cis isomers by Lincoln and Stranks.[2] There are no major differences, and there does not appear to be any obvious correlation with the ^{31}P chemical shifts.

2. Kinetic Data for Isomerization. Figure 6 gives spectrophotometric traces as a function of time for reaction of the trans complex at pH 2.20 and 25 °C, $I = 1.0$ ($NaClO_4$). Isobestic points are almost maintained at 560 and 445 nm. Table III collects rate

Table II. Acidity Constants (pK_a) for *trans*- and *cis*-$[Co(en)_2(OH/H)(OPO_3/H/H)]^{2+,+,0}$ Ions in 1.0 mol dm^{-3} $NaClO_4$ at 25 °C

complex	pK_a trans	pK_a cis[a]
$[Co(en)_2(OH_2)(OPO_3H_2)]^{2+}$	3.17 ± 0.08[b]	3.10 ± 0.05[b]
$[Co(en)_2(OH_2)(OPO_3H)]^+$	6.6 ± 0.2[c]	6.75 ± 0.05[c]
$[Co(en)_2(OH)(OPO_3H)]$	9.27 ± 0.06[d]	9.40 ± 0.05[d]

[a] Data reported in ref 2. [b] pK_{a1}. [c] pK_{aq}. [d] pK_{a2}.

Table III. Rate Data[a] for the Isomerization of the Trans Complex at 25.0 °C, I = 1.0 mol dm^{-3} ($NaClO_4$)

pH	$10^5k_{obs}/s^{-1}$	pH	$10^5k_{obs}/s^{-1}$
0 (1 M $HClO_4$)	4.15	5.51[c]	20.0
1 (0.1 M $HClO_4$)	4.90	5.99[e]	20.3
2 (0.01 M $HClO_4$)	7.22	6.52[e]	16.3
2.98[b]	12.4	7.00[e]	11.0
3.53[b]	19.0	7.49[f]	7.70
3.97[b]	21.0	7.98[f]	3.43
4.51[c]	20.7	8.49[f]	2.50
5.01[c]	21.3	9.01[f]	1.48
5.05[d]	20.5	9.51[g]	1.70

[a] Spectrophotometric data, 505 nm. [b] 0.05 M HEPES buffer. [c] 0.05 M acetate buffer. [d] 0.10 M acetate buffer. [e] 0.05 M MES buffer. [f] 0.05 M Tris buffer. [g] 0.05 M CAPS buffer.

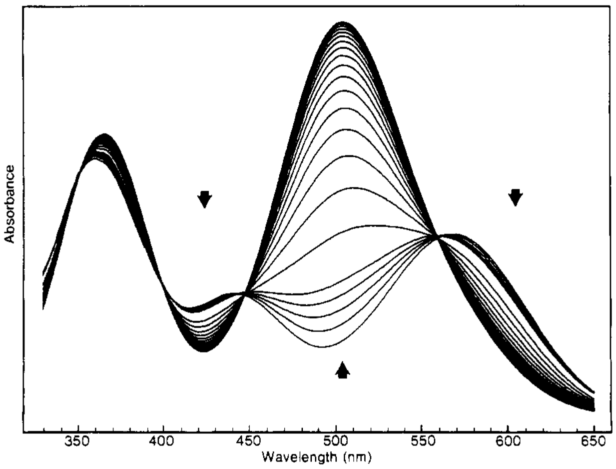

Figure 6. Repetitive visible–UV spectra (650–330 nm) for the reaction of *trans*-$[Co(en)_2(OH_2)(OPO_3H_2)]^{2+}$ at pH 2.20, I = 1.0 M ($NaClO_4$), 25.0 °C. The first five spectra were obtained at 15-min intervals, and the remainder were obtained at 60-min intervals.

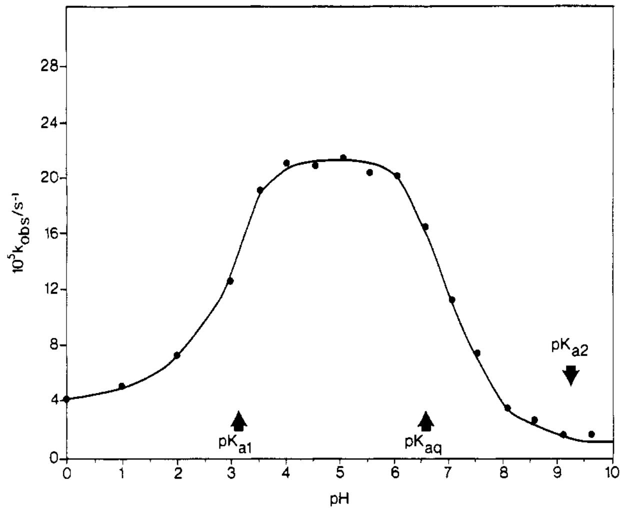

Figure 7. Plot of k_{obs} vs pH for reaction of the trans-monodentate phosphate complex at 25.0 °C, I = 1.0 M ($NaClO_4$). Spectrophotometric rate data were collected at 505 nm.

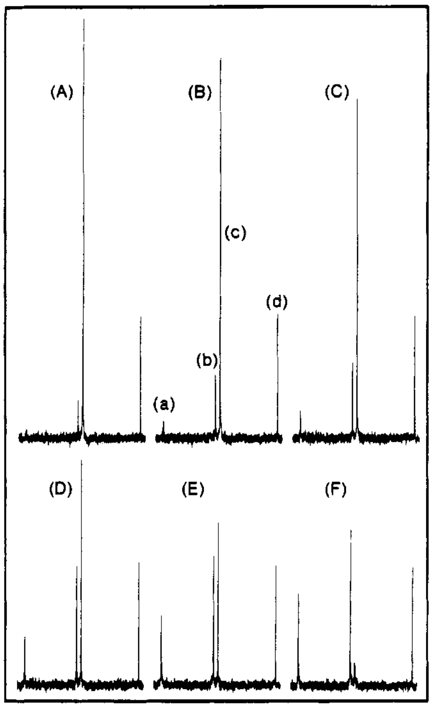

Figure 8. Selected ^{31}P NMR spectra from a kinetic experiment starting with *trans*-$[Co(en)_2(OH_2)(OPO_3H_2)]ClO_4{\cdot}H_2O$ (77.8 mg dissolved in 3.1 cm^3 of 0.2 M MES buffer containing 20% D_2O) at pH 6.0. Acquisitions were spaced 16 min apart (256 transients; delay time 2 s) starting ~10 min after mixing. Peaks represent (a) chelate, (b) cis-monodentate complex, (c) trans-monodentate complex, and (d) external reference (0.1 M H_3PO_4). Key: (A) first spectrum; (B) spectrum after 16 min; (C) spectrum after 32 min; (D) spectrum after 96 min; (E) spectrum after 144 min; (F) spectrum after 10 h.

data from several such experiments at different pHs. No buffer dependence (acetate) was found. Good first-order plots were obtained in the acid to neutral pH range but for the slower runs (pH 7.98–9.51) Guggenheim plots were used to obtain k_{obs}. The wavelength chosen for data collection (505 nm) maximized the absorbance change (increase) but did not allow an obvious choice to be made between the two possible immediate products, the cis-monodentate and chelate complexes. Indeed, the absorptivity difference between these two species is not large at any wavelength (Figure 2 shows differences in acidic solution, and they are even less in alkali[1]), and this combined with the large absorbance change from the trans reactant does not allow a choice to be made. In acidic solution (pH <4), the final product (at equilibrium) is entirely the cis-monodentate one (^{31}P spectra), but since opening up of the chelate is much faster than the present reaction under this condition, the chelate could conceivably be the immediate product. However, the rate of reaction of the trans complex maximizes between pH 4 and 6 (Figure 7), and under this condition the cis → chelate rate is similar (k_{obs} = 2.0 × 10^{-4} s^{-1}).[3] Also at pH 6, the chelate assumes significant proportions at equilibrium. Under this condition, ^{31}P NMR spectra allow the immediate reaction product to be identified. Figure 8 shows portions of a kinetic experiment at pH 6.0. Early spectra show a rapid buildup of the cis-monodentate complex with the chelate lagging behind; that is, the cis/chelate ratio is larger at early times than later on. Thus the sequence trans → cis → chelate holds for reaction of *trans*-$[Co(en)_2(OH_2)(OPO_3H)]^+$ at pH 6. It is expected (but cannot be proved) that this sequence also holds for reaction of *trans*-$[Co(en)_2(OH_2)(OPO_3H_2)]^{2+}$ in the more acidic pH range mentioned above.

In alkaline solution (pH >9.5) the trans-hydroxo complex is very slow to react and complete loss of phosphate to give $[Co(en)_2(OH)_2]^+$ and HPO_4^{2-}/PO_4^{3-} competes with isomerization and complicates spectrophotometric traces. Under such circumstances, ^{31}P NMR spectra again allow the sequence of events to be unraveled since the growth and decay of each phosphate-containing species can be separately monitored. Figure 9 shows selected

Table IV. ^{31}P NMR Rate Data for the Reaction of Phosphate Complexes in Buffered Alkaline Solution at 25.0 °C, $I = 1.0$ M ($NaClO_4$ or $NaNO_3$)

			k_{obs}/s^{-1} for formation of		
pH	0.1 M buffer	reactant complex	chelate	cis-monodentate complex	trans-monodentate complex
11.29	NEt_3	chelate		2.5×10^{-4}	6.8×10^{-6}
11.1	NEt_3	cis-monodentate	1.5×10^{-4}		6.6×10^{-6}
10.82	NEt_3	trans-monodentate	1.0×10^{-5}	$\sim 1 \times 10^{-5}$	
10.8	NEt_3	chelate		1.8×10^{-4}	$<5 \times 10^{-6}$
10.1	CAPS	cis-monodentate	3.2×10^{-4}		$<5 \times 10^{-6}$
9.9	CAPS	chelate		*a*	$\sim 2 \times 10^{-6}$[b]
8.95	TAPS	trans-monodentate	2.0×10^{-5}	*a*	

[a] Too little formed for a rate to be obtained. [b] Estimated from $t_{1/2} \simeq 100$ h.

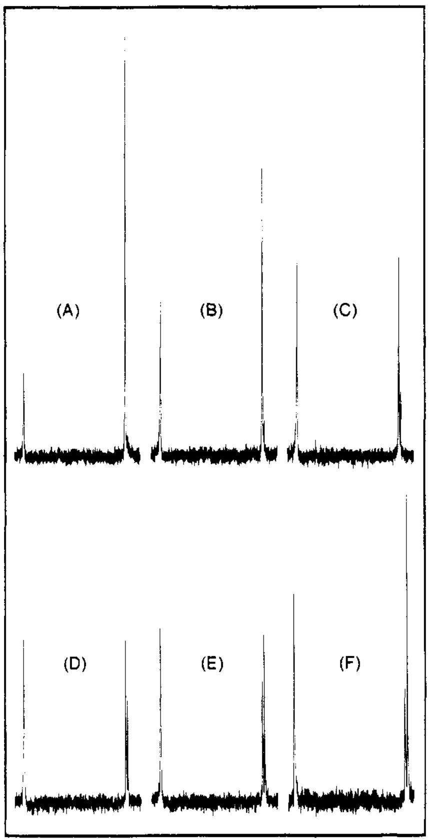

Figure 9. Parts of selected ^{31}P NMR spectra from a kinetic experiment starting with *cis*-$[Co(en)_2(OH_2)(OPO_3H_2)](ClO_4)_2$ (100 mg dissolved in 3.5 cm^3 of 0.2 M CAPS buffer containing 20% D_2O, $I = 1.0$ M ($NaClO_4$)) at pH 11.1. Acquisitions (512 transients; delay time 2 s) were spaced at appropriate time intervals with those shown representing (A) the first acquisition starting ~10 min after mixing and acquisitions (B) after 2 h, (C) after 6 h, (D) after 14 h, (E) after 28 h, and (F) after 60 h (this last spectrum is at a different amplitude).

spectra from a kinetic experiment at pH 11.1 starting with *cis*-$[Co(en)_2(OH)(OPO_3)]^-$ as the reactant. The signal representing the chelate grows in first reaching its equilibrium value after about ~10 h, while at longer times the absorption representing *trans*-$[Co(en)_2(OH)(OPO_3)]^-$ continues to grow. This reaches its equilibrium value after about 1 week. A plot of the separate integrated absorptions as a function of time is given in Figure 10. It can be seen that the cis → chelate reaction is considerably faster at this pH than the cis → trans reaction. Rate data from several such experiments using different starting complexes are collected in Table IV. When the initial reactant was the chelate, the cis-monodentate complex always appeared first followed at longer time by the trans-monodentate complex. Thus the (reverse) sequence trans → cis → chelate must hold under these alkaline conditions. It was also clear from the kinetic experiment carried out at pH 8.95 (TAPS, buffer, Table IV) that formation of the chelate starting with the trans reactant is controlled by the rate of formation of the cis intermediate.

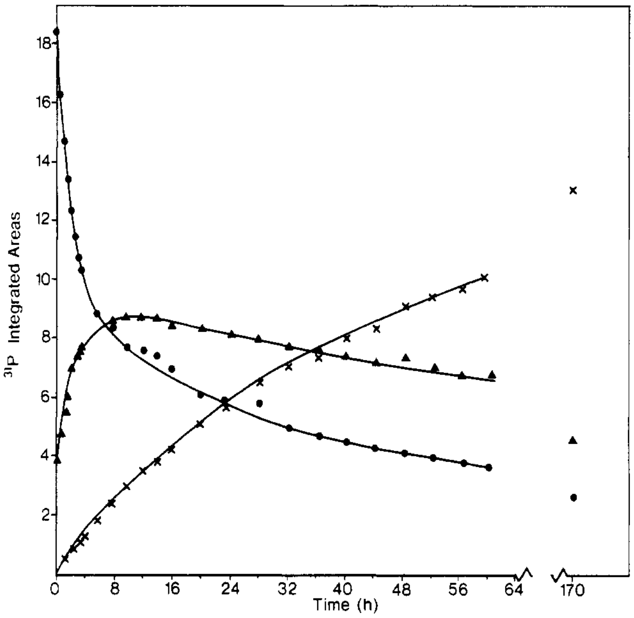

Figure 10. Plot of ^{31}P NMR integrated intensities vs time for the reaction of *cis*-$[Co(en)_2(OH)(OPO_3)]^-$ at pH 11.1 (256 or 512 transients; 2-s time delay between transients): (●) cis reactant; (▲) chelate product; (×) trans product.

Table V. Equilibrium Concentrations[a] of Chelate, Cis-Monodentate, and Trans-Monodentate Complexes as a Function of pH (25.0 °C, I = 1.0 mol dm^{-3} ($NaClO_4$ or $NaNO_3$) from ^{31}P NMR Spectra

		integrated signal intens[b]			ratios	
pH	0.1 M buffer	chelate	cis	trans	chelate/cis	trans/cis
6.48	TES	2.50	0.92	0	2.7	0
7.23	TES	4.47	0.37	0.11	12.1	0.30
7.83	TES	4.49	0.20	0.14	22.5	0.70
8.40	TAPS	4.19	0.17	0.12	24.7	0.71
8.90	TAPS	4.10	0.16	0.17	25.6	1.06
9.62	CAPS	4.09	0.16	0.41	25.6	2.56
9.90	CAPS	3.42	0.22	0.59	15.6	2.68
10.14	CAPS	2.82	0.30	1.02	9.4	3.40
10.23	NEt_3	2.72	0.27	1.14	10.1	4.22
10.82	NEt_3	1.28	0.47	1.94	2.7	4.13
10.95	NEt_3	1.03	0.50	2.05	2.1	4.10
11.38	NEt_3	0.41	0.63	2.47	0.65	3.92
11.56	NEt_3	0.27	0.57	2.49	0.47	4.37
12.21	NEt_3	0	0.61	2.31	0	3.79

[a] Standard mixtures of the three complexes showed that integrated areas are representative of concentrations when a 3-s time delay is used between acquisitions. After 16 days at 25.0 °C. [b] Relative to an external reference of 0.1 M H_3PO_4 (0.0 ppm): 512 or 1024 transients, pulse width 10 μs, acquisition time 0.791 s, delay 3.000 s.

3. Equilibrium Measurements. ^{31}P NMR spectra were used to determine the equilibrium concentrations (1, 2, and 5 weeks at 25 °C) of the chelate, cis-monodentate, and trans-monodentate complexes, over the pH range 6.48–12.21. Selected spectra have been given previously,[1] and data from a new set (using an external

0.1 M H_3PO_4 standard) are given in Table V. Under the conditions [Co] = 5.02×10^{-2} mol dm^{-3}, 0.1 mol dm^{-3} buffer, I = 1.0 M ($NaClO_4$), and 25.0 °C, significant amounts of free phosphate were also present at equilibrium (as demonstrated by similar spectra after 2 and 5 weeks), but these values are not reported here due to the absence of appropriate standards.

Discussion

It is apparent that the final products at equilibrium originating from the four-membered phosphate chelate under alkaline conditions are somewhat more complicated than was originally proposed by Lincoln and Stranks.[2-4,10] The appearance of a trans-monodentate isomer parallels in many respects that found for the oxalate system,[6,7] although in the present case all acts of bond breaking occur at the Co(III) center rather than at the ligand P(V) atom.[1,5] The overall processes involved can be separated into four pH regions appropriate to the various protonated forms of the reactants.

(i) Acidic Solution (pH <3). Under this condition the cis-monodentate $[Co(en)_2(OH_2)(OPO_3H_2)]^{2+}$ is the only product at equilibrium. Both the trans-monodentate complex and the chelate convert into it in a first-order manner but at very different rates. That for the *trans*-$[Co(en)_2(OH_2)(OPO_3H_2)]^{2+}$ complex is rather slow, $k_0{}^t = 4 \times 10^{-5}$ s^{-1} (25 °C, I = 1.0 mol dm^{-3}), but that for the chelate is fast. Lincoln and Stranks[3] report a rate $k_0{}^{ch} = 0.4 \pm 0.1$ s^{-1} at 10 °C and I = 2.5 mol dm^{-3}, and we have remeasured this as 1.67 s^{-1} at 25.0 °C and I = 1.0 mol dm^{-3} ($NaClO_4$) using a stopped-flow spectrophotometer. It is not known whether the trans complex converts directly to the cis complex or whether the reaction occurs via the unstable chelate, but clear evidence at other pHs (eq 5) suggest the direct path. If so, the rate 4×10^{-5} s^{-1} would measure the rate of water exchange provided every act of recoordination gives rise to the cis-aqua complex. This is likely in view of the absence of any trans complex at equilibrium and could be easily verified by using ^{17}O NMR spectroscopy.

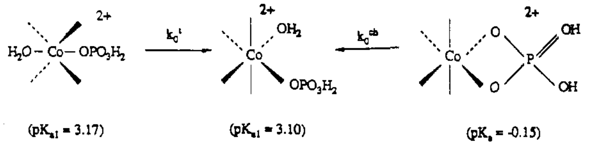

(5)

$$k_0{}^t = 4 \times 10^{-5}\ s^{-1} \qquad k_0{}^{ch} = 1.67\ s^{-1}$$

(ii) Acid–Neutral Solution (pH 3–7). Under this condition, the cis-monodentate complex is again the most stable at equilibrium but with an increasing presence of the chelate as the pH approaches 7. Lincoln and Stranks' equilibrium and kinetic data[3] give a good account of the overall processes in this region. The rate of conversion of *trans*-$[Co(en)_2(OH_2)(OPO_3H)]^{1+}$ to the cis isomer maximizes here (Figure 7), and at equilibrium there is little or no (<1%) trans species present. ^{31}P NMR spectra (Figure 8) clearly implicate the cis complex as the intermediate in the conversion of the trans-monodentate complex to the chelate. This implies that reaction of the trans complex is again controlled by ligand–solvent water exchange rather than by direct entry of phosphate oxygen since the latter would directly give the chelate. The rate and equilibrium data may be summarized as follows:

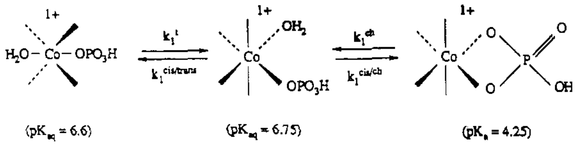

(6)

$$k_1{}^t = 2.08 \times 10^{-4}\ s^{-1} \qquad k_1{}^{ch} = 5.7 \times 10^{-3}\ s^{-1}$$

$$k_1{}^{cis/trans} = 0 \qquad k_1{}^{cis/ch} = 2.2 \times 10^{-4}\ s^{-1}$$

$$K_1{}^{trans/cis} = 0 \qquad K_1{}^{ch/cis} = 0.04$$

(iii) Mildly Alkaline Solution (pH 8–10). Here the chelate is stabilized, but it is still in measurable equilibrium with both the trans- and cis-monodentate species. The interconversion rates for chelate → cis ($k_2{}^{ch}$) and cis → trans ($k_2{}^t$, $k_2{}^{cis/trans}$) are not very different so these processes interfere with each other in kinetic experiments starting with the chelate. Both the rate data starting with the trans isomer (Table IV) and ^{31}P NMR spectra for the reverse reaction show that the cis isomer is again the intermediate in conversion of the trans isomer to the chelate. Under this condition, the rate and equilibrium data can be summarized as follows:

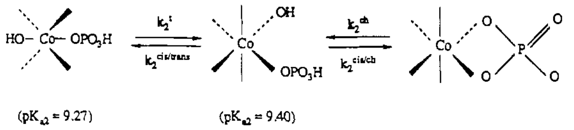

(7)

$$k_2{}^t = 2 \times 10^{-5}\ s^{-1} \qquad k_2{}^{ch} = 2.2 \times 10^{-5}\ s^{-1}$$

$$k_2{}^{cis/trans} = 1 \times 10^{-5}\ s^{-1} \qquad k_2{}^{cis/ch} = 6 \times 10^{-4}\ s^{-1}$$

$$K_2{}^{trans/cis} \simeq 0.5 \qquad K_2{}^{ch/cis} \simeq 25$$

(iv) Strongly Alkaline Solution (pH >10). Under this condition, the chelate becomes increasingly unstable (in a first order in [OH^-] manner), and the trans-monodentate isomer is more stable than the cis by about 4:1. The cis-monodentate isomer is again the intermediate in the conversion of the chelate to the trans isomer. Opening up of the chelate is slower by a factor of ~100 than was originally proposed,[3] but it is still faster than formation of the trans isomer from the cis. No first order in [OH^-] path could be detected for the latter reaction up to 0.1 M OH^-. The equilibrium and kinetic data are as follows:

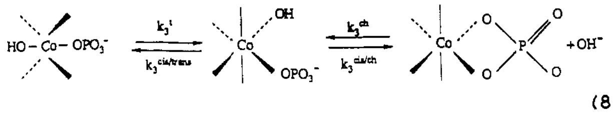

(8)

$$k_3{}^t \simeq 1.3 \times 10^{-6}\ s^{-1} \qquad k_3{}^{ch} = 1.75 \times 10^{-2}\ mol^{-1}\ dm^3\ s^{-1}$$

$$k_3{}^{cis/trans} \simeq 5.4 \times 10^{-6}\ s^{-1} \qquad k_3{}^{cis/ch} = 7.5 \times 10^{-5}\ s^{-1}$$

$$K_3{}^{trans/cis} = 4.1 \qquad K_3{}^{ch/cis} = 4.3 \times 10^{-3}\ mol\ dm^{-3}$$

Complete Hydrolysis and Reanation by Phosphate. This aspect was not studied in detail in this investigation although it was clear from the ^{31}P NMR spectra that free $HPO_4{}^{2-}/PO_4{}^{3-}$ had accumulated after 2 and 5 weeks (25 °C) and that these solutions had reached an equilibrium condition. Lincoln and Stranks studied the hydrolysis reaction in strong alkali[10] and found it to be very slow. Our observations agree with this and extend it to the less alkaline regions (to pH ~7). Probably both the trans- and cis-monodentate complexes undergo hydrolysis, but since their interconversion is somewhat faster than hydrolysis, the details of this reaction will prove difficult to unravel. Likewise, Lincoln and Stranks[4] studied the reanation reaction over the pH range 4–9 and interpreted their results in terms of anation of *trans*-$[Co(en)_2(OH)(OH_2)]^{2+}$ by ion-paired $HPO_4{}^{2-}$ (they report a rate for *trans*-$[Co(en)_2(OH)(OH_2)]^{2+}HPO_4{}^{2-}$ of k_{an} = 0.255 min^{-1} at 47.9 °C). Our results show that equilibrium is also reached under more alkaline conditions (to pH 12.1 at least), and the amounts of *trans*- and *cis*-$[Co(en)_2(OH)_2]^+$ and $HPO_4{}^{2-}/PO_4{}^{3-}$ species that must be present under these conditions suggest that ion-pairing involving these reactants is also involved in the anation process. However, we do not intend looking at these processes further.

Acknowledgment. We wish to thank Dr. W. T. Robinson for the X-ray data collection.

Supplementary Material Available: Table S1, containing ^{31}P NMR frequencies, and Tables S2 and S3, containing bond lengths, bond angles, and calculated H atom positions and thermal parameters (4 pages). Ordering information is given on any current masthead page.